Study of Sub-Wavelength Gratings to Understand their Polarization Behaviour

Gayathri M S*, Anil Prabhakar, and Shanti Bhattacharya
Indian Institute of Technology Madras, Department of Electrical Engineering
*Corresponding author: Photonics Group, Department of Electrical Engineering, Indian Institute of Technology Madras, Chennai - 600036, India, gayathrims@ee.iitm.ac.in

Abstract: In this paper, we explore the use of COMSOL for studying sub-wavelength gratings. This software appears ideal for this application as it is capable of solving Maxwell's vectorial equations with appropriate boundary conditions. In addition, it demonstrates the polarization dependent behaviour of such gratings. The model developed uses an incident plane wave and Floquet periodicity as a boundary condition to replicate a unit cell. The parameters, calculated from earlier work, of the polarizing beam splitting grating, are verified in this paper with 2-dimensional transmission grating models. The diffraction efficiencies of the transverse electric and transverse magnetic orders obtained, affirm the validity of the simulation.

Keywords: sub-wavelength gratings, polarization splitting, Floquet periodicity.

Figure 1. 2-D view of a grating that splits TE and TM components into different orders. h,n - height and refractive index of the grating, d - period, a/d - fill factor, and θ_B - incident Bragg angle.

1. Introduction

Phase gratings are used in many applications due to their high diffraction efficiencies. With sub-wavelength dimensions, the behaviour of a simple binary phase grating becomes polarization dependent[1], as shown in Figure 1. One way of characterizing such a grating is to calculate the diffraction efficiency. In this case, this involves calculating the efficiency with which the transverse electric (TE) and transverse magnetic (TM) components have been separated. COMSOL™ is based on finite element modelling and is chosen for two reasons; firstly, because it can handle complex 2-D and 3-D geometries and secondly, it can handle the vector nature of the fields associated with these structures. The objective of the design work carried out in this paper is to compare the results of a commonly used analytical method with those obtained with the FE model of COMSOL™.
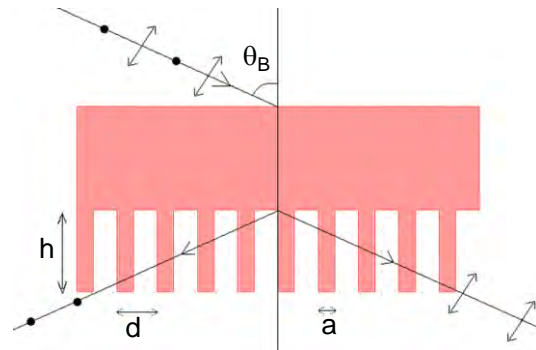
2. Theory

In a grating with large feature sizes, light is diffracted into different spatial locations (or orders) that can be derived based on scalar theory. When the dimensions of the structure become comparable to or less than the wavelength of light, the structural details cannot be resolved and the number of diffraction orders are reduced. With careful design, it is possible to create a structure that allows only the 0th order to propagate. All higher orders become evanescent. In such a case, the structure can even be approximated to a homogeneous medium[1] of some effective index to which Snell's laws can be applied; albeit with some special properties. The uniqueness lies in the anisotropy of the structure which introduces a "form" birefringence[2]. Hence, light is split in two different directions, apparently producing orders again. This behaviour occurs when the angle of incidence satisfies the Bragg condition. Because of the polarization sensitivity of a sub-wavelength grating, the TE and TM components separate into two different orders. One of the main factors determining the efficiency of this separation is the grating height.

3. Use of COMSOL Multiphysics

COMSOL™ Multiphysics 3.5a with MATLAB™ offers a great deal of flexibility for computing diffraction efficiencies in the far-field in addition to the ease and accuracy with which it solves for structures of even sub-wavelength dimensions. It also offers support in the visualization of the polarization sensitivity of these gratings.

3.1 The Physical Model

The RF module of COMSOL™ is used to simulate the propagation of a 650 nm plane wave incident on a simple two-level phase grating. A 2-D geometry, as shown in Figure 2, is constructed to create a cross section of a one dimensional grating.
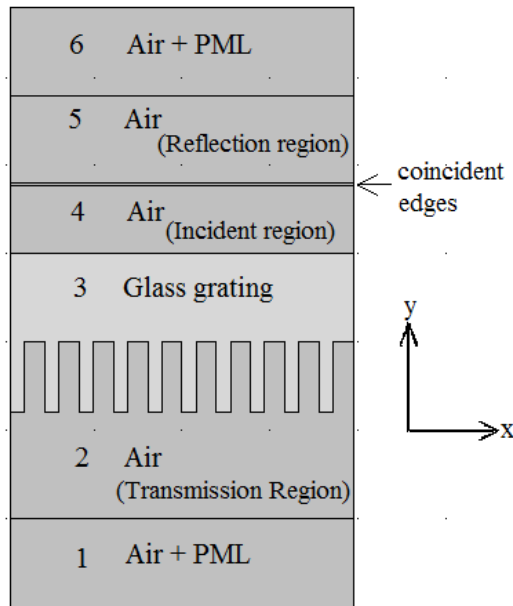

Figure 2. 2-D geometry describing the various domains of the one dimensional binary phase grating model.

A special assembly of edges, connecting regions 4 and 5, is used to filter out only the reflected light into region 5. The incident medium will contain the fields that excite the model as well as the fields that are reflected from the grating; whereas the reflection region will have only the reflected light without the incident

light. To allow for high transmission, the grating line widths are taken to be of the same material as that of the substrate, which is a glass material of refractive index 1.457. The diffracted fields that couple out of the grating propagate forward into the transmission region. The air domain in which the grating is held, is padded in the y-direction with a special air region called perfectly matched layer (PML) of large enough thickness so as to avoid any non-physical reflections. In the model described above, the grating dimensions for the two case studies taken up for simulation are as tabulated in Table 1 and the thickness of the rest of the sub domains are taken to be about 1 micron each. The transmission grating described in the paper is modelled for these two sets of data; PBS-A for a Bragg incidence of 56° and PBS-B for 45°.

Table 1: Parameters used in the simulation, following Ferstl et al[3]

	Grating Period, d[nm]	Line width, a[nm]	Grating height, h[nm]
(PBS-A)	390	160	790
(PBS-B)	460	140	930

3.2 The Mathematical Model

The RF module solves for the electric and magnetic fields from Maxwell's vector wave equation in each node of the finite element model. Hence the governing equation is

$$\nabla \times \mu_r^{-1}(\nabla \times \vec{E}) - k_0^2(\varepsilon_r - \frac{j\sigma}{\omega\varepsilon_0})\vec{E} = \vec{0} \quad (1)$$

where $k_0 = \omega\sqrt{\mu_0\varepsilon_0}$ and the symbols have their usual meanings. Maxwell's equations are solved in all the sub-domains of different materials in the model. For our refractive index model, the assumptions based on the material properties are $\mu_r = 1$, $\sigma = 0$ and $\varepsilon_r = n^2$. Hence (1) reduces to

$$\nabla \times (\nabla \times \vec{E}) - k_0^2 n^2 \vec{E} = \vec{0}, \quad (2)$$

where n is the refractive index of the material. No electromagnetic loss in the media further

constrains the index from having an imaginary part. A harmonic propagation analysis solves for the dependent variables, $\vec{E}_z$ and $\vec{H}_z$.

3.3 Boundary Conditions

The mathematical model is incomplete without adding constraints that actually introduce continuity or discontinuity in the electric and magnetic field solutions at the mesh nodes in the interface between two media.

PML matches the impedance with its neighbouring domain and self absorbs all the fields that come into it. This works for a wide range of angles of incidence and mimics an infinite space in the y-direction as in real space.

The effect of an infinite grating is achieved by the use of Floquet boundary condition. This condition mimics the multiple structures that are required to accurately model diffraction, saving memory and computational time. Hence it is used to flank the model from the sides as shown in Figure 3. Floquet harmonics are used to evaluate the field in the grating taking into account the phase shift that is introduced by the structure between the ends along $\hat{x}$, which is the direction of periodicity.
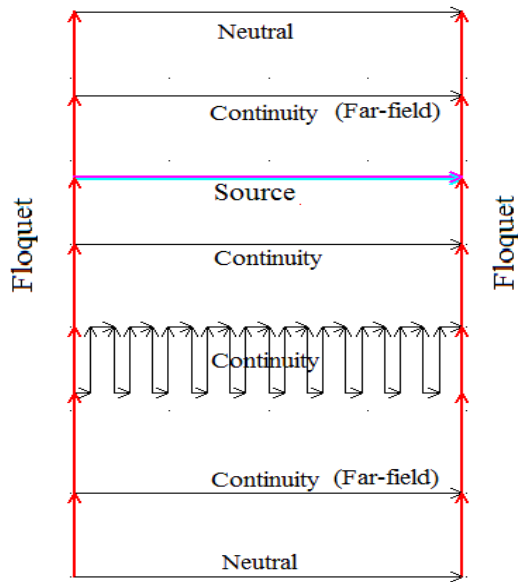

Figure 3. Boundary constraints

An "identity pair" of ports for excitation ensures the extraction of the reflection spectrum that would be required for studying reflection gratings. These are two overlapping boundaries whose physics is connected by the port boundary condition for excitation. The source is excited with a linearly polarized light that is a combination of TE (electric field along z-direction) and TM (magnetic field along z-direction) components. It is assumed that the electric field makes 45° with the grating grooves so that the incident electric field polarization is composed equally of TE and TM components. Hence, $\vec{E}_z$ and $\vec{H}_z$ make up the incident hybrid field.

$$\vec{E}_z = \hat{e}_z \, E_0 \, \cos\theta \exp(-j(k_x x - k_y y)) \quad \textbf{(3)}$$

$$\vec{H}_z = \hat{e}_z \, H_0 \, \sin\theta \exp(-j(k_x x - k_y y)) \quad \textbf{(4)}$$

where

$$\theta = 45^o \quad (5)$$

E_0 and H_0 are the field amplitudes in air,

$$H_0 = E_0/\eta_0$$

$\eta_0 = 377 \ \Omega$, is the characteristic impedance of air, and k_x and k_y are the components of the incident wave vector.

A neutral boundary condition was imposed on the boundaries, as seen in Figure 3, which reflects the out of plane E- and H- fields, though it may be argued that strictly such a boundary condition is not necessary after a PML.

All the other interior boundaries should of course mandate continuous solutions. Most importantly, the far-field is user-defined in a variable, say 'EFar', at the transmission and reflection ends labelled as 'Far-field' in Figure 3. The x, y and z components of the electric field at the far-zone are computed in EFarx, EFary and EFarz. Though the far-field variables are defined in these boundaries, a surface plot of these variables over the entire domain gives a sense of the direction of the diffraction orders.

3.4 Finite Element Model

Meshing requires care especially when there are periodic conditions involved. The mesh nodes of the Floquet edges are the exact copies of their phase shifted counterparts. To resolve the wavelength finely enough with the mesh, the maximum element size of the triangular mesh is chosen as one-tenth of the wavelength in the

medium. The statistics related to the mesh are given in Table 2.

Table 2: Mesh statistics

	PBS-A	PBS-B
Element shape	Triangular	Triangular
Number of Mesh elements	23114	27084
Number of degrees of freedom	93420	109400
Minimum element quality	0.8561	0.8544
Maximum element size in air domain	65 nm	65 nm
Maximum element size in glass domain	43 nm	43 nm

The analysis is carried out for a sweep of incident angles from 0° to 90° . We also did a parametric analysis to observe the trend of polarization sensitivity and diffraction efficiency at Bragg incidence and at other incidence.

The direct (PARDISO) linear solver is used. The calculation time is about 25 minutes on a 2.4 GHz processor with 2GB RAM.

4. Results

The hybrid incident plane wave that splits into the TE and TM components along different directions is clearly observed in the surface plots shown in Figures 4 and 5. The plots show the electric field resulting from a beam incident at the Bragg angle. We observe, from Figure 4, that the TE component is entirely transmitted and diffracted; while the TM component, in Figure 5, is both reflected and transmitted into the corresponding 0th orders.

Therefore, a linearly polarized wave incident at Bragg angle on a grating with sub-wavelength period would selectively get diffracted into a particular direction depending on whether it was a TE or TM wave.
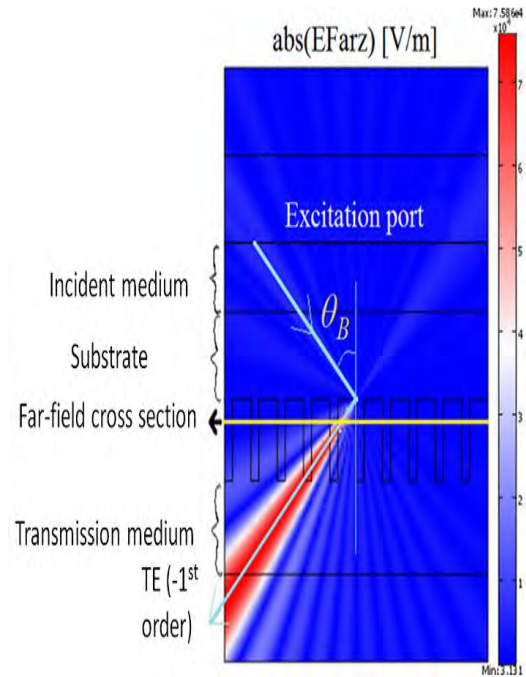

Figure 4. Direction of far field for TE component at Bragg incidence for PBS-B
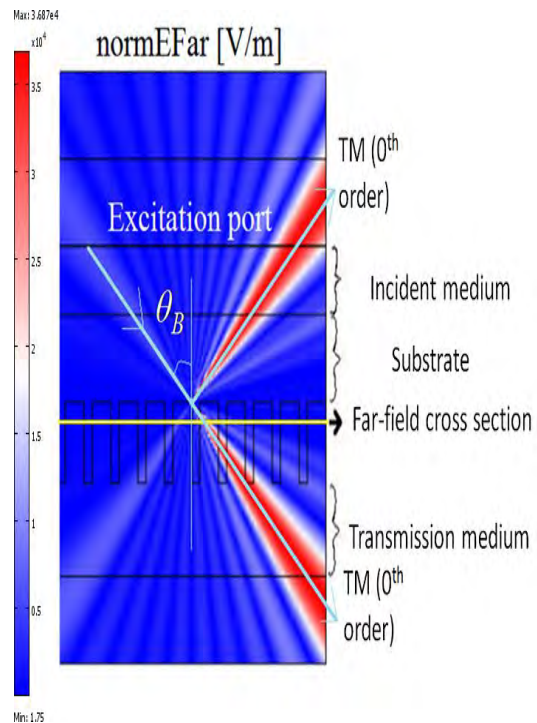

Figure 5. Direction of far field for TM component at Bragg incidence for PBS-B

This is shown, in Figures 6a and 6b, for the design PBS-A in the far-field transmission zone. Similar curves are obtained for PBS-B. Note that the Bragg angle for PBS-A is 56° and for PBS-B is 45°. To get the diffraction efficiency of an order, an integration of the predefined COMSOL™ variables, normEFar^2 or abs(EFarz)^2, over sections of the far-field cross section were evaluated. The command "meshintegrate" is used in the FE model object in MATLAB™ to perform an integration over an arbitrary cross section.
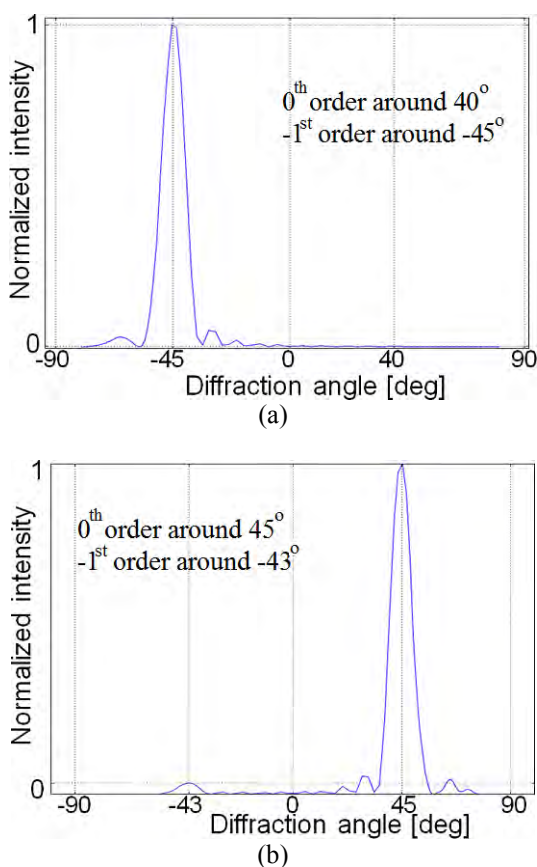

(a)

(b)

Figure 6. Transmitted far E-field distribution for PBS-B design at Bragg incidence of 45° with plots of (a) TE component and (b) TM component

The far-field cross sections, shown in Figures 4 and 5, are taken at a suitable y distance from the grating such that arc-tangent of the (x/y) covers diffraction angles between -90° and 90°. This calculation of the y distance is depicted in Figure 7.
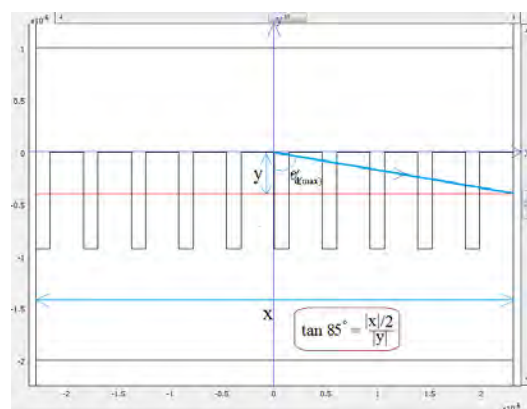

Figure 7. Optimum y distance such that $\theta_{d(\max)} = \pm 85^o$ at which far-field power is calculated

The far-field power thus calculated is normalized with respect to the power in the transmission spectrum in the entire cross section. Table 2 compares the diffraction efficiencies obtained from the Ferstl model[3] with those obtained from our model.

Table 2: Comparison of theoretical and simulated diffraction efficiencies for PBS-A and PBS-B designs evaluated at Bragg incidence

	Ferstl[3]	COMSOL
PBS-A		
TM 0	99.7%	95%
TE -1	93.6%	92.9%
PBS-B		
TM 0	95%	89.1%
TE -1	92%	92.3%

5. Conclusions

The aim of this paper was to understand how efficiently and easily, COMSOL could be used to study sub-wavelength structures. This was tested by taking already reported structures and modelling them in COMSOL. In general, the way to use COMSOL would be to initially design the structure, i.e., calculate its dimensions using an existing diffraction model (e.g., modal method[4]), and then analyse the field patterns using COMSOL.

Our results show that calculations of diffraction efficiencies of sub-wavelength gratings obtained using COMSOL were found to match earlier results. Hence, COMSOL can be

relied upon for vector models such as sub-wavelength gratings and for far-field calculations. Also, the model can be extended to complex geometries where the mathematics becomes more complex and the field patterns harder to visualize.

6. References

1. Philippe Lalanne and Jean-Paul Hugonin, *High-order effective-medium theory of subwavelength gratings in classical mounting: application to volume holograms,* J. Opt. Soc. Am. A 15, 1843-1851 (1998).
2. M. Born and E. Wolf, *Principles of Optics*, 705-708, 6th ed. (Pergamon Press), New York, (1980).
3. Margit Ferstl, Ralf Steingrueber, Daniel Dias, Svetomir Stankovic and Helmut Haidner, *High-frequency gratings as polarization elements,* Proc. SPIE 3879, 138 (1999).
4. Juan Liu, Hua Gao, Jing Zhou, *The design of a polarizing beam splitter made from a dielectric rectangular-groove grating,* Optics & Laser Technology 41, 622-626 (2009).